Indian Journal of Engineering & Materials Sciences
Vol. 14, February 2007, pp. 12-18

Flow characteristics in a transition duct passing from rectangular section to circular section

Hasan Gül[a]* & Duygu Evin[b]

[a]Vocational High School, [b]Mechanical Engineering Department, Fırat University, 23119, Elazıg, Turkey

Received 25 November 2005; accepted 8 November 2006

The characteristics of a flow in a transition duct, in which the flow passes from a rectangular cross-section to a circular one, were investigated experimentally. The transition duct had an entry aspect ratio of 0.65 and exit aspect ratio of 1. The experiments were conducted at three different channels which have different lengths. The exit cross-sectional area of the transitional duct was double of the inlet. Reynolds number varied in the range of 2×10^5-6×10^5. Local pressures and velocities were measured along the duct.

IPC Code: G01F1/05

Pipes having same or different cross-sectional areas are used for transition ducts which are known as "transition pipes" or "transition fittings". This type of pipes can be seen at current machines and pipe line network. Ducts with non-circular cross-sections are also frequently encountered in industrial heat transfer equipment such as compact heat exchangers, cooling channels in gas turbine blades, ventilation and turbo machinery. Because of practical importance, the flow dynamics and heat transfer in rectangular ducts have received continuous attention during past several decades[1].

Chiu and Seman[2] have reported that square duct may be used to replace the traditional circular pipes for the transport of solids. The cause for the reduction in head loss has been attributed to the formation of secondary current. There have been extensive researches on the turbulent flow characteristics in several kinds of rectangular ducts with rough walls, and have presented detailed distributions of the primary and secondary flow velocities, turbulent intensities, and turbulent shear stresses over the duct cross-section[3-6]. Gessner and co-workers[7,8] provided experimental data for square ducts for several Reynolds numbers. Further discussions on experiments and calculation methods for flow in non-circular ducts involving turbulence driven secondary motions are found[9,10]. Constant-extensional rate or transitions channel systems have become a rapidly developing technology, finding applications in many areas of engineering and science[11].

*For correspondence (E-mail: hgul@firat.edu.tr)

There is enough information in the open literature about the flow characteristics in pipes. However, in many applications ducts those have different geometries and cross-sections are used. Consequently, a transition duct is needed as a joining element so as to pass from a cross-section to another.

The purpose of this study is to provide detailed information in a transition channel in which the flow passes from a rectangular duct to a circular one- in the turbulent flow. Flow characteristics of this duct of interest in engineering applications were investigated, experimentally.

Experimental Procedure

The experimental set-up shown in Fig. 1 consists of a turbo fan, an orifice, an entry-section for providing fully developed flow, a test-section in which the measurements are taken and an exit-section for preventing the effects of the ambient on this turbulent flow.

Shlichting[12] and Fox and McDonalds[13] suggest that a fully developed velocity profile exist after an inlet length of the 25-40 diameters. An inlet pipe of 3000 mm length, which is about 27 channel hydraulic diameters, provided a fully developed turbulent flow before this transition channel. Consequently, for a fully developed flow, air drawn from a turbo fan passes through a constant entry-section that has a 130×200 mm cross-sectional area and 3000 mm length. A transition duct from a rectangular duct to a circular pipe is located just after the entry-section. The inlet rectangular and the exit circular cross-sectional areas of the test-section were A_1 = 130×200

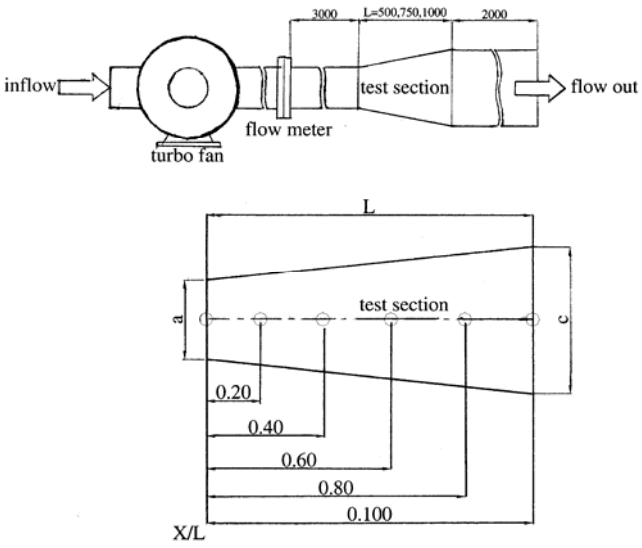

Fig. 1 — Experimental set-up

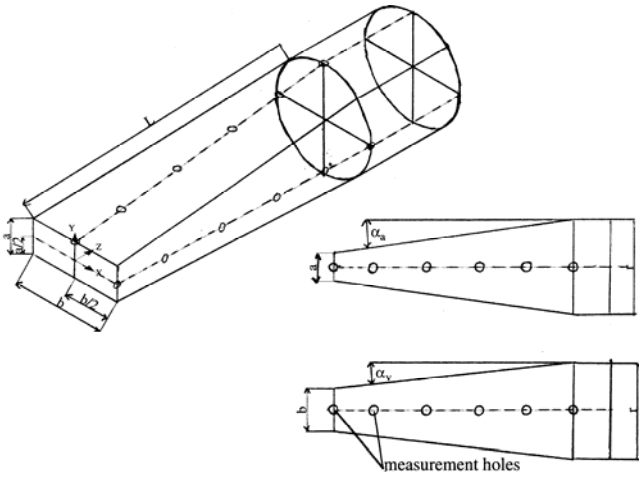

Fig. 2 — Details of the transition channel

Table 1 — Properties of the transition channel

Re = 2×10^5-6×10^5					
L (mm)	ϕ (°)	α_v (°)	α_a (°)	A_1 (m^2)	A_2 (m^2)
500	5	7	7		
750	5	7	7	0.026	0.0519
1000	5	7	7		

= 0.026 m^2 and $A_2 = \pi(0.02573)^2/4 = 0.0519$ m^2, respectively. The equivalent conical angle of the channel was $\phi = 5°$. As can be seen in Fig. 2, the divergence angle between the lateral side and the z-axis was chosen as $\alpha_a = 7°$ and the divergence angle between the bottom wall and the z-axis was $\alpha_v = 7°$. Both of the opposite walls were symmetrical to each other. Three different transition ducts with 500, 750 and 1000 mm length were used in the experiments, respectively. All the transition ducts used in the experiments had an entry aspect ratio of 0.65 and exit aspect ratio of 1. While the rectangular entry cross-sectional dimension of the transition ducts was 130×200 mm, the circular exit diameter was 257 mm. The exit cross-sectional area of the transitional duct was double of the inlet. The parameters used in the experiments are shown in Table 1.

So as to measure the pressure and velocity distributions along the transition duct, holes were drilled to the top and lateral sides of the transition duct at the z/L=0.0, 0.20, 0.40, 0.60, 0.80, 1.00 points, as seen in Fig. 2. The local pressure and velocity values were scanned for each aforementioned z/L points on y-axis between $0 \le y/(a/2) \le 1$ and x-axis between $0 \le x/(b/2) \le 1$ with 5 mm intervals. Consequently, the pressure and velocity distribution from the center to the lateral and top wall of the channel were measured, respectively. The Dantec Streamline constant temperature anemometry system was used for the velocity measurements. Measurements were acquired with a model 55P11 single normal hot-wire probe. Himanshu *et al.*[14] and Hirota *et al.*[15] also used hot-wire anemometers so as to measure velocity distributions in rectangular ducts.

The uncertainty of measurements was estimated using method given by Moffat[16]. The uncertainty in Reynolds number was ±2%, friction factor was about ±4.5%, and average velocity was %1.1.

An important parameter to define the transition channels having different cross-sectional areas and geometries is the equivalent conical angle. The equivalent conical angle ϕ can be calculated follows[17,18]

$$\tan\phi = \frac{dr}{dz}; \quad \tan\phi = \left(\frac{R_1}{2.l}\right)\frac{f_1(\psi,\beta,\gamma) + 2.f_2(\psi,\beta,\gamma).\bar{z}}{\sqrt{\bar{A}_z}} \qquad \ldots(1)$$

where Ψ, β, $\bar{z}$ and γ, A_z dimensionless parameters can be defined as

$$\bar{A}z = \frac{A_z}{A_1} = 1 + f_1(\psi,\beta,\gamma).\bar{z} + f_2(\psi,\beta,K).z^2 \qquad \ldots(2)$$

$$\gamma = \frac{A_2}{A_1} \qquad \ldots(3)$$

$$\psi = \frac{a}{b} \qquad \ldots(4)$$

$$\beta = 1 \qquad \ldots(5)$$

$$\overline{z} = \frac{z}{L} \qquad \ldots(6)$$

The function of $f_1(\psi,\beta,\gamma)$ was found[17,18] and $f_2(\psi,\beta,\gamma)$ is calculated as follows:

$$f_2(\psi,\beta,\gamma) = \gamma - 1 - f_1(\psi,\beta,\gamma) \qquad \ldots(7)$$

The Reynolds number Re and the friction factor, *f*, are defined as follows respectively,

$$\mathrm{Re} = \frac{\rho U.D_h}{\mu} \qquad \ldots(8)$$

$$f = \frac{\Delta P}{4(1/D_h)(1/2)\rho_{air}U^2} = \frac{1}{2}\Delta P\frac{D_h}{\rho_{air}U^2} \qquad \ldots(9)$$

The calculated friction coefficient is compared with Petukhov friction factor[19] which is valid for $4000 \le \mathrm{Re} \le 5.10^6$.

Results and Discussion

The velocity distributions at *x* and *y* axes along the channel are shown in Figs 3-8. In Figs 3-8, because of the axial symmetry the pressure and velocity measurements were taken at the stations from the channel axis to the channel walls along the diverging channel as shown in Fig. 2. It is obvious that velocity values increase with the increasing flow rates. It is also clear in these figures that, increasing axial cross-sectional area along the channel because of the divergence causes a decrease in velocity. There also exists a sharp velocity decrease close to the walls because of the boundary layer. However, the velocity couldn't be measured so close to the wall due to the limited access of the velocity meter.

The local velocity distribution along the channel (z/L=0.20, 0.40, 0.60, 0.80, 1.00) which has an equivalent angle of 5°, length of 500 mm and divergence angle of α_v=7° is shown in Fig. 3 for four Re numbers. At each z/L point the velocity values are scanned laterally for $0 \le x/(b/2) \le 1$ *x*-direction. Because the change in cross-sectional area is so small in the inlet zone of the channel especially at z/L=0.20, the decrease in velocity is much smaller than it is at the downstream of the channel. Since the channel's

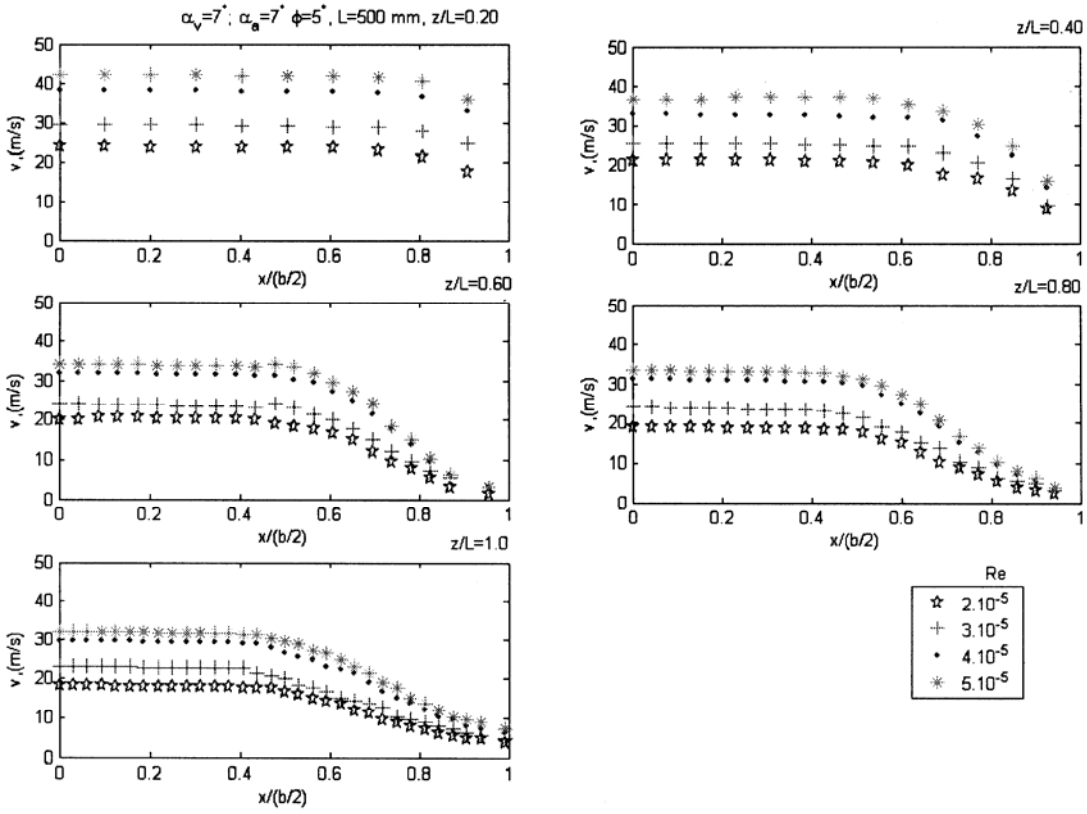

Fig. 3 — Velocity distributions at *x*-axis ($0 \le x/(b/2) \le 1$) along the channel (z/L=0.20-1.00)

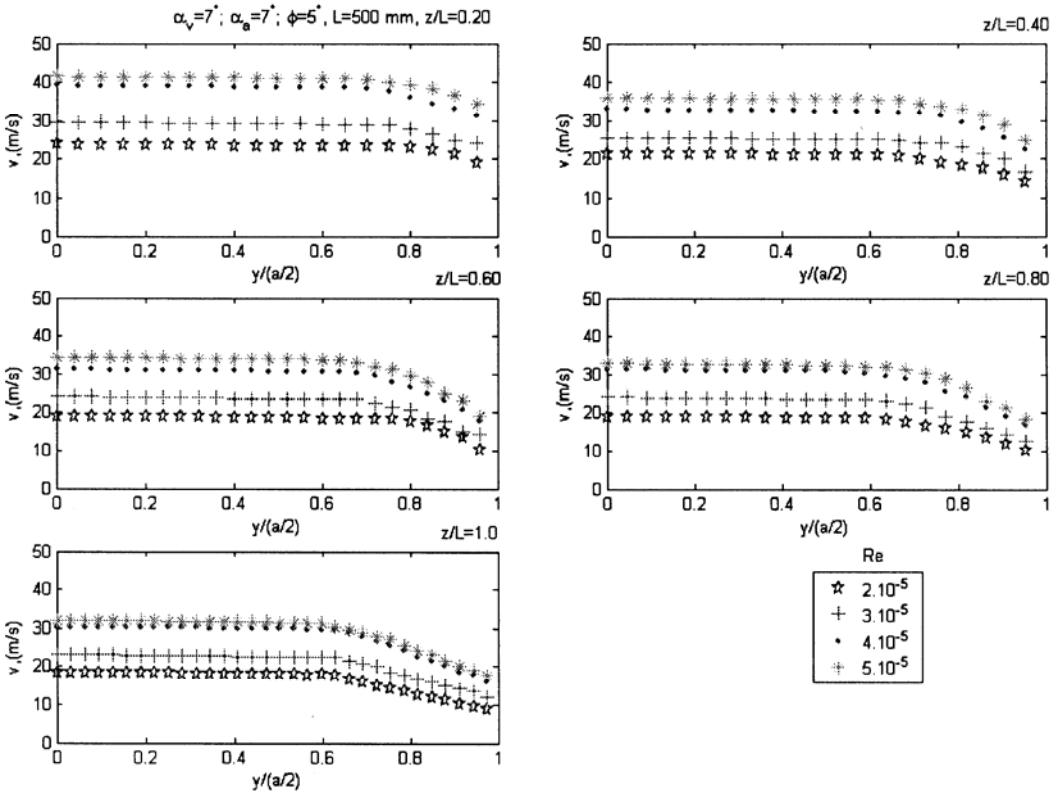

Fig. 4 — Velocity distributions at *y*-axis ($0 \leq y/(a/2) \leq 1$) along the channel (z/L=0.20-1.00)

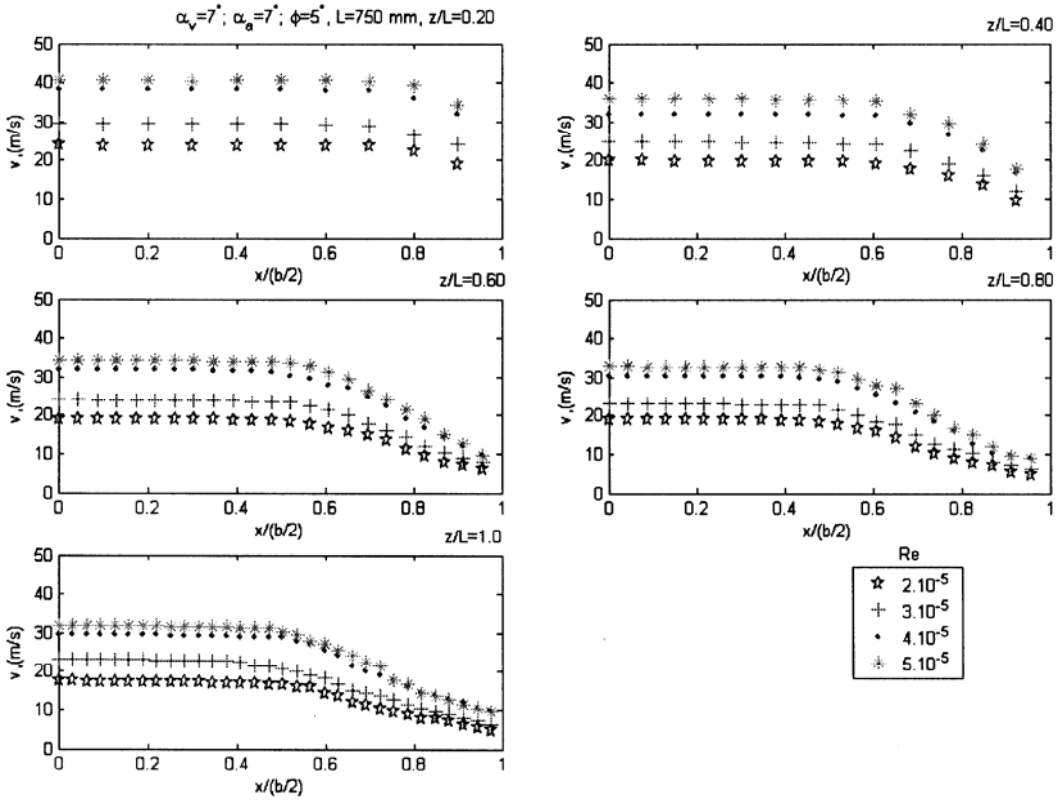

Fig. 5 — Velocity distributions at *x*-axis ($0 \leq x/(b/2) \leq 1$) along the channel (z/L=0.20-1.00)

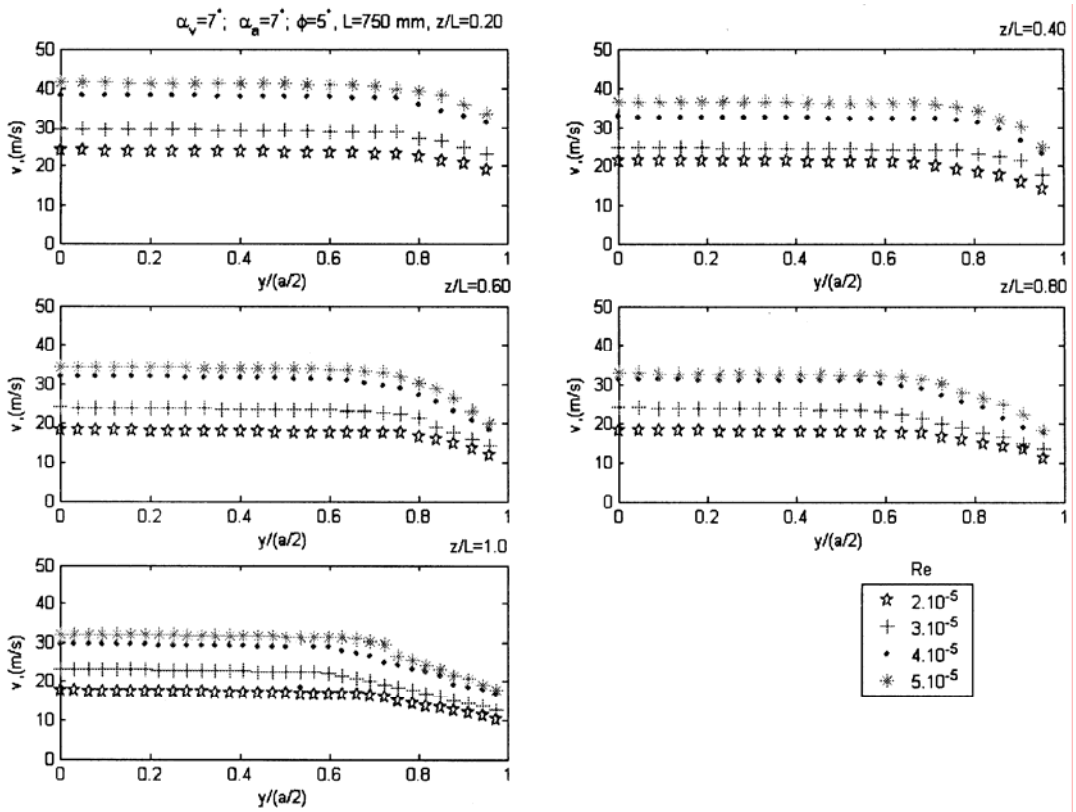

Fig. 6 — Velocity distributions at y-axis ($0 \leq y/(a/2) \leq 1$) along the channel (z/L=0.20-1.00)

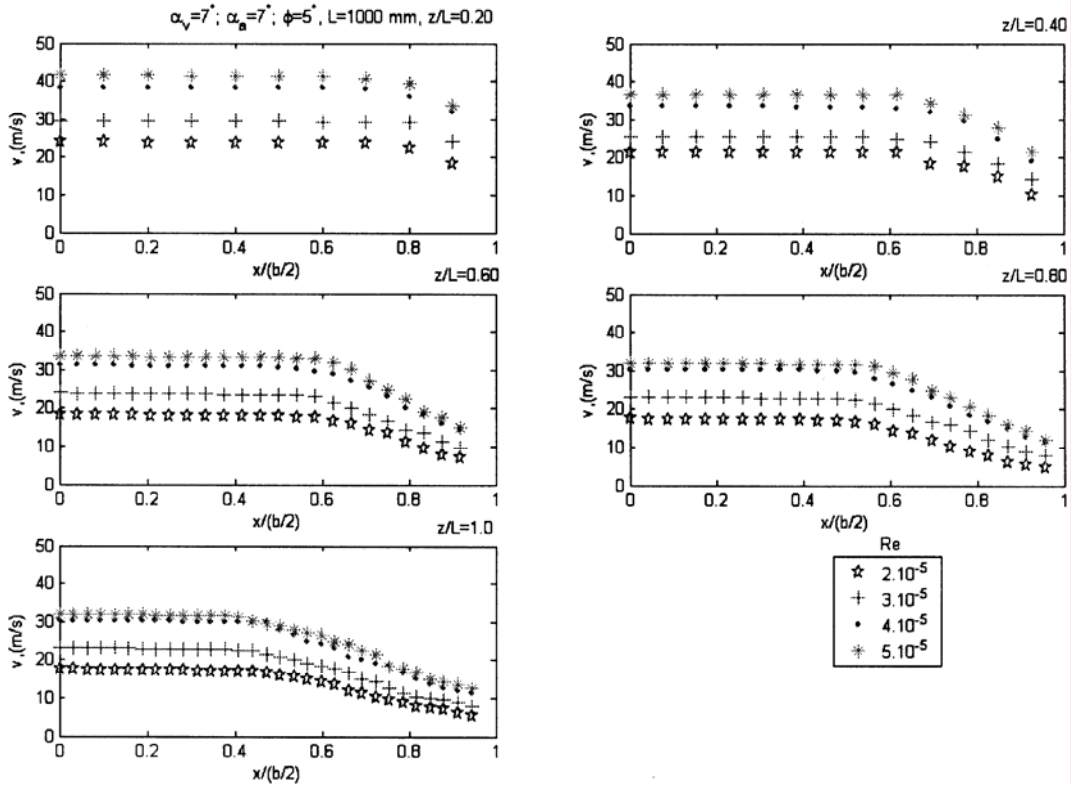

Fig. 7 — Velocity distributions at x-axis ($0 \leq x/(b/2) \leq 1$) along the channel (z/L=0.20-1.00)

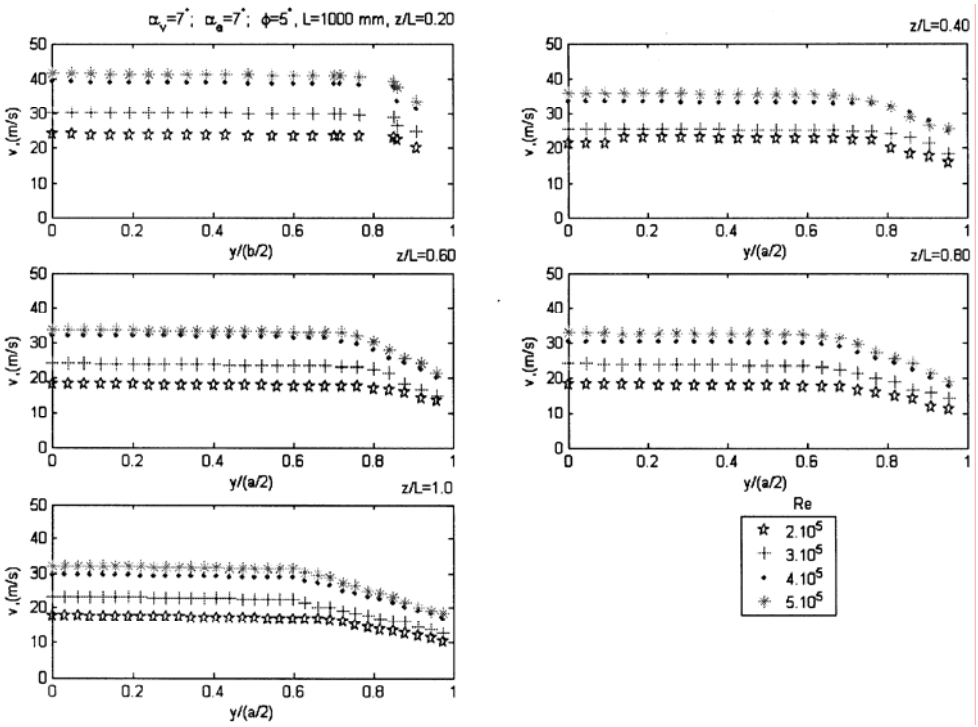

Fig. 8 — Velocity distributions at *y*-axis ($0 \le y/(a/2) \le 1$) along the channel (z/L=0.20-1.00)

geometry changes from rectangular to circular and an extension exists, a sharp velocity decrease occurs near to the exit of the transition channel for each Re number.

The local velocity distribution along the channel (z/L=0.20, 0.40, 0.60, 0.80, 1.00) which has an equivalent angle of 5°, length of 500 mm and divergence angle of α_a=7° is shown in Fig. 4. At each z/L point the velocity values are scanned vertically for $0 \le y/(a/2) \le 1$ at *y*-direction. The similar tendencies in the curves in Fig. 3 can be seen in this figure, too. However, the decrease in velocity near the exit isn't as sharp as it is at *x*-direction. This may depend on divergence angle which is smaller.

The local velocity distribution along the channel (z/L=0.20, 0.40, 0.60, 0.80, 1.00) which has an equivalent angle of 5°, length of 750 mm and divergence angle of α_v=7° is shown in Figs 5 and 6. The effect of channel length is investigated in these figures. The transition channel is longer. Since there exists a sudden geometrical change from rectangular to circular in the short channel (L=500 mm), the velocity decrease is sharper than the channel of 750 mm. Velocity curves show that there exist cross flows especially about the exit where the geometry changes from rectangular to circular. However, these cross flows slightly straighten with the increasing Re number.

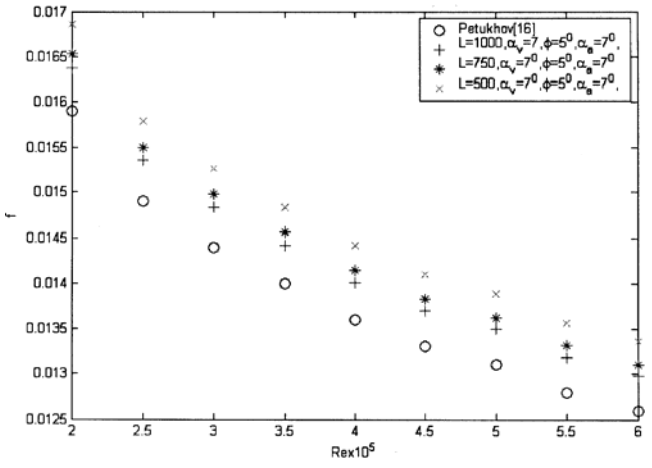

Fig. 9 — Friction factor versus Re number for different channel lengths

The local velocity distribution belonging to the transition channel with the same angles but which has a length of 1000 mm can be seen in Figs 7 and 8. This is the longest transition channel being investigated. The velocity values especially near the exit section are higher and the declining curve near the exit section is straighter when compared to the aforementioned shorter transition channels.

The relation between friction factor and Reynolds number is shown in Fig. 9 for all three transition ducts. The bulk velocity which is related to the mass

flow is used for calculating the Darcy friction factor. It is obvious that friction factor is decreasing with the increasing Reynolds number and increasing channel length. The friction factor belonging to the shortest channel is the highest which may depend on the smaller transition cross-section and rapid geometry change at the shortest channel. The calculated friction factor is compared with the Petukhov's in this figure. The difference between this experimental study and the Petukhov correlation may occur because of the geometrical and cross-sectional change.

Nomenclature

A_1 = inlet cross-sectional area, m^2
A_2 = exit cross-sectional area, m^2
D_h = hydraulic diameter of the channel, m
f = friction factor
L = length of the tube, m
Re = Reynolds number
U = average velocity, m/s
ΔP = pressure gradient across the channel, N/m^2

Greek symbols

μ = dynamic viscosity of air, kg/msn
υ = kinematics viscosity of air, m^2/s
ρ = density of air, kg/m^3
α_a = divergence angle between the lateral sides and the z-axis, 7°
α_v = divergence angle between the bottom or top walls and the z-axis, 7°
ϕ = equivalent conical angle, 5°
Ψ = a/b
β = 1

References

1 Ito H, *JMSE Int J,* 30 (1987) 543-552.
2 Chiu C L & Seman J, in *Advances in solid-liquid flow in pipes and its application,* edited by Zandi I (Pergamon Press, UK), 1971, 16.
3 Yokosawa H, Fujita H, Hirota M & Iwata S, *Int J Heat Fluid Flow*, 10 (1989) 125-130.
4 Fujita H, Yokosawa H & Hiroto M, *Exp Therm Fluid Sci,* 2 (1989) 72-80.
5 Fujita H, Hiroto M, Yokosawa H, Hasegawa M & Gotoh I, *JMSE Int (Ser II)*, 33 (1990) 692-701.
6 Hiroto M, Fujita H, Yokosawa H & Tanaka Y, *Turbulence Heat Mass Transfer,* 1 (1995) 512-519.
7 Gessner F B & Jones J B, *J Fluid Mech*, 23 (1965) 689-713.
8 Gessner F B & Emery A F, *ASME J Fluid Eng*, 103 (1981) 445-455.
9 Demuren A O & Rodi W, *J Fluid Mech*, 140 (1984) 189-222.
10 Demuren A O, *AIAA J*, 29 (1990) 531-537.
11 Shirakashi M, Ito H & James D F, *J Non-Newtonian Fluid Mech*, 74 (1998) 247-262.
12 Schlichting H, *Boundary layer theory* (McGraw-Hill, New York), 1979.
13 Fox R W & McDonalds A T, *Introduction to fluid mechanics*, (Wiley, New York), 1994.
14 Tyagi H, Liu R, Ting D S-K & Johnston C R, *Exp Therm Fluid Sci,* 30 (2006) 587–604.
15 Hirota M, Fujita H & Yokosawa H, *J Phys E Sci Instrum*, 21 (1988) 1077-1084.
16 Moffat R. J, *Exp Therm Fluid Sci*, 1 (1988) 3-17.
17 Dekam E I & Calvert J R, *J Wind Eng Ind Aerodyn,* 24 (1986) 117-127 .
18 Dekam E I & Calvert J R, *J Wind Eng Ind Aerodyn,* 18 (1985) 275-286 .
19 Incropera F P & DeWitt D P *Fundamentals of heat and mass transfer,* 4th ed (John Wiley & Sons Inc., New York), 1996.